PREPARATION AND TRIBOLOGICAL PROPERTIES OF $W_{0.97}Mo_{0.03}Se_2$ NANOSHEETS

XIANGHUA ZHANG[a,b], DU ZHANG[c], HONGTAO ZHANG[c], HUA TANG[c], CHANGSHENG LI[b,c*], YUE JIN[c]

[a]*School of Mechanical Engineering, Jiangsu University of Technology, Changzhou 213001, Jiangsu Province, China*

[b]*School of Mechanical Engineering, Jiangsu University, Key Laboratory of Tribology of Jiangsu Province, Zhenjiang 212013, Jiangsu Province, China*

[c]*School of Materials Science and Engineering, Jiangsu University, Zhenjiang 212013, Jiangsu Province, China*

The $W_{0.97}Mo_{0.03}Se_2$ nanosheets have been successfully prepared by a facile reaction in closed reactor at moderate temperature. The thermal (750°C) solid-state reaction between the ball-mixed of micro-sized selenium, tungsten and molybdenum powders yielded a high yield of $W_{0.97}Mo_{0.03}Se_2$ nanosheets. The as-prepared products were characterized by XRD, SEM, and TEM. SEM images showed that the morphologies of the as-prepared products changed with the reaction temperature and duration. The tribological properties of the as-prepared products as additives in the HVI500 base oil were investigated by UMT-2 multispecimen tribotester. The friction coefficient of the base oil containing $W_{0.97}Mo_{0.03}Se_2$ nanosheets was lower and more stable than that of the base oil.

(Received November 5, 2013; Accepted December 19, 2013)

Keywords: nanosheets, solid-sate reaction, tribological properties

1. Introduction

In order to increase the mechanical efficiency and reduce the friction and wear of lubricated contacts, an appropriate additive should be added to avoid surface damage. Many studies [1-5] have proved that lubrication additives affect the performance characteristics of lubricant greatly. Layered materials such as graphite, MoS_2 and WS_2, which are often used both as solid lubricants and as additives in liquid lubricants, had been extensively studied and used for a long time [6-9].

Recently, some researchers had focused on the tribological properties of the transition-metal diselenide as lubrication additive, which had the similar structure to the MoS_2 and WS_2. For example, Yang et al. [10] investigated the tribological properties of WSe_2 nanorods as additives in HVI500 base oil and demonstrated that the friction coefficient of the base oil containing WSe_2 nanorods was decreased. Cao et al. [11] fabricated ultrathin WSe_2 nanosheets with tower-like structure and researched their tribological properties as additive added into paraffin. Li et al. [12] synthesized $NbSe_2$ fibers and investigated their tribological behavior. It was found that the addition of a small amount (5 wt.%) of the $NbSe_2$ fibers significantly decreased the friction coefficient of N46 engine oil. Tang et al. [13] investigated the tribological properties of the

*Corresponding author: lichangshengujs@yahoo.com

as-prepared $NbSe_x$ powders as additives in HVI500 base oil. In order to further improve the tribological properties of lubricating oil additive, a recent innovative technique involves the doping of the transition-metal dichalcogenides with cations and anions. For example, Efeoglu et al. [14] investigated the tribological properties of MoS_2-Nb solid lubricant composite film. Recently, we have reported the synthesis of Mo-doped WSe_2 nanolamellars [15] and Nb-doped $MoSe_2$ nanoplates [16] and researched their tribological propertied as additive added into the base oil. It was found that the obtained product with the contents of dopant within 3-5 at% showed the best friction performance.

In this study, we reported a facile and efficient solid-state reaction method for the synthesis of $W_{0.97}Mo_{0.03}Se_2$ nanosheets using tungsten, molybdenum and selenium powders at 750 ^oC in an argon atmosphere. Moreover, the influences of the reaction temperature and duration on the morphology of the $W_{0.97}Mo_{0.03}Se_2$ nanosheets were investigated. And the tribological properties of $W_{0.97}Mo_{0.03}Se_2$ nanosheets as additives in the HVI500 base oil were also investigated.

2. Experimental

2.1 Materials

High-purity selenium, tungsten and molybdenum powders were purchased from Shanghai Chemical Reagent Co. Ltd. (Shanghai, China). All chemical reagents were of analytic purity and used directly without further purification.

2.2 Preparation of $W_{0.97}Mo_{0.03}Se_2$ nanosheets

In a typical procedure, high-purity tungsten, molybdenum and selenium powders (molar ratio: W:Mo:Se = 97:3:220, an overdose of 10% Se) were mixed in the steel kettle (ball: material = 20:1) and mechanically milled at 300 rpm (rotation per minute) for 12 h in a planetary ball mill. Then the ball-milled mixture was introduced into 10-ml stainless steel reactor in a nitrogen-filled glove box. The filled reactor was tightly closed with the threaded plug and pushed into the tube furnace. The temperature of the tube furnace was raised to 750 ^oC at a rate of 10 $^oC\ min^{-1}$ and the temperature was maintained at 750 ^oC for 1h. Subsequently the reactor was gradually cooled to room temperature, opened, and the as-prepared powder was obtained. The product was directly characterized without further processing by various analytic techniques.

2.3 Characterization methods

The X-ray diffraction (XRD) patterns were recorded using a D8 advance (Bruker-AXS) diffractometer with Cu *Ka* radiation (λ = 0.1546 nm). The 2θ range used in the measurement was from 10 to 80° with a velocity of 5° min^{-1}. The morphologies and structures of the samples were characterized by scanning electron microscopy (SEM, JEOL JXA-840A) and transmission electron microscopy (TEM) with a Japan JEM-100CX II transmission electron microscope.

Friction tests were performed using a UMT-2 ball-on-disc tribometer (CETR, USA) under lubricated conditions. The as-prepared $W_{0.97}Mo_{0.03}Se_2$ powder modified by dispersing agent sorbitol monooleate (Span-80) was distributed into the HVI500 base oil via 60 min ultrasonication, leading to the desired samples with different contents of $W_{0.97}Mo_{0.03}Se_2$. The testing of friction reduction and wear resistance was conducted at rotating speed of 400 rpm and load of 6-60 N for 12 min. The material of upper sample is 440C stainless steel ball with a diameter of 10 mm, hardness of 62 HRC, and the counterpart is 45 steel disc of Φ40 mm×3 mm in size. The friction coefficient was automatically recorded during the contact friction.

3. Results and discussion

3.1 Structure and morphology characterization

The overall crystal structure and phase purity of the $W_{0.97}Mo_{0.03}Se_2$ nanosheets were examined by XRD. As shown in Fig. 1a, it can be seen that the XRD pattern of the $W_{0.97}Mo_{0.03}Se_2$

nanosheets is similar to that of hexagonal WSe_2, indicating that the $W_{0.97}Mo_{0.03}Se_2$ nanocrystals has been well synthesized. All the diffraction peaks correspond well to the hexagonal phase (p63/mmc space group) of WSe_2 with lattice constants a = 3.286 Å and c = 12.983 Å (PDF No. 38-1388). And no evidence of any other phases were detected indicating that the product is of high purity. The XRD pattern clearly shows that (002) reflection is of the maximum intensity and thereby indicates the presence of a well-stacked layered structure.

The morphologies of the as-fabricated products were identified by SEM. Fig. 1b shows a low-magnication SEM image of the sample, and it can be seen that the sample is composed of some conelike microrods. The magnified SEM image of the microrod (Fig. 1c) clearly shows that it was composed of numerous nanosheets.

TEM and high-resolution TEM (HRTEM) studies were carried out to provide detailed descriptions of the morphology and crystallinity of the $W_{0.97}Mo_{0.03}Se_2$ nanocrystals. As observed in Fig. 1d, the thickness of the nanoplates is ~10 nm. Fig. 1e is the HRTEM image of $W_{0.97}Mo_{0.03}Se_2$ nanocrystals. The lattice fringes have an interplanar distance of 0.65 nm, which is consistent with the (002) crystal planes of hexagonal WSe_2.

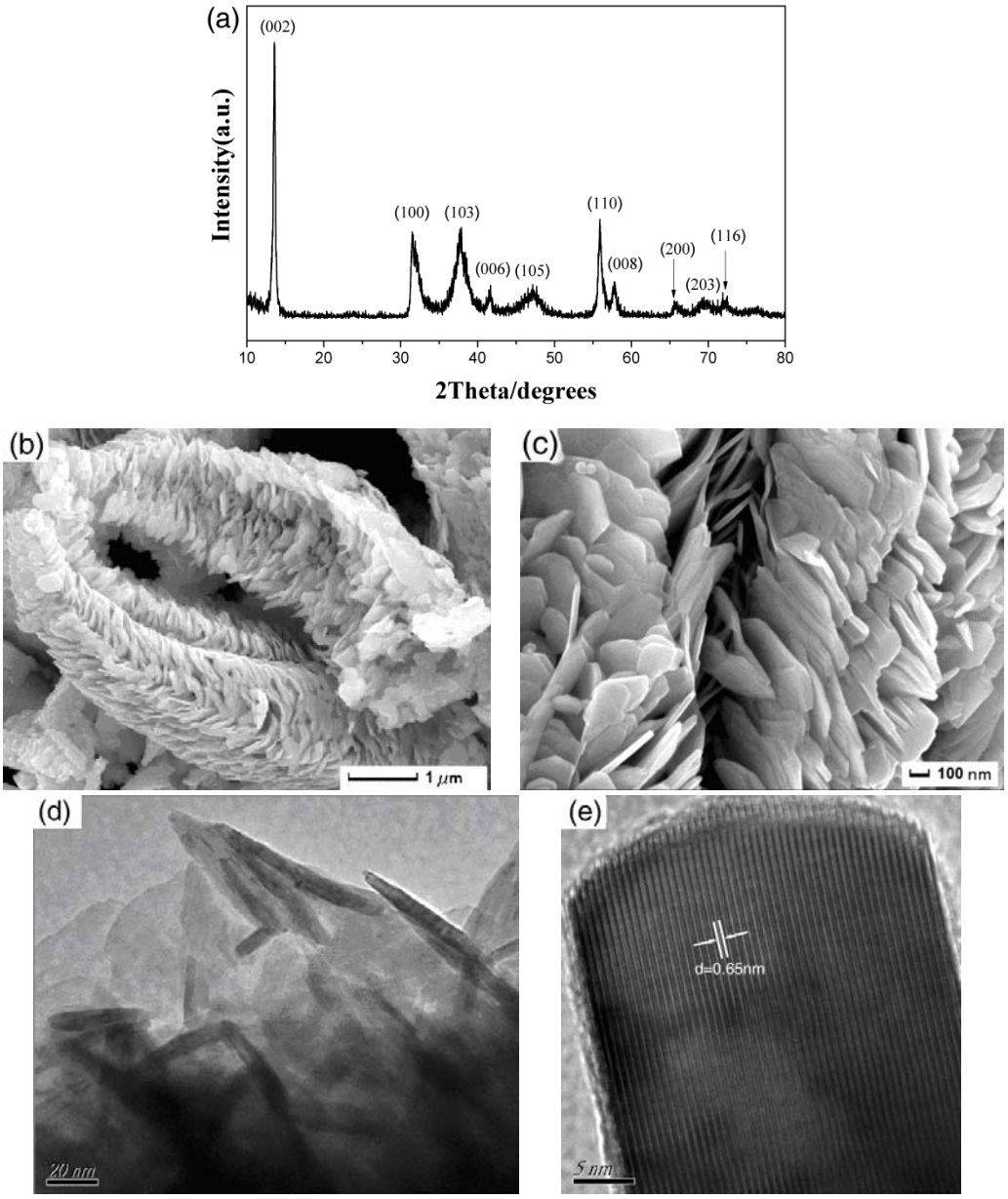

Fig. 1. (a) XRD pattern, (b) , (c) SEM, (d) TEM and (e) HRTEM images of the as-prepared $W_{0.97}Mo_{0.03}Se_2$ nanosheets.

3.2 Influences of the reaction temperature and duration

A series of experiments have been carried out to investigate the influence of reaction temperature and time on the morphology of the final products. The influence of temperature was investigated from 600-900 ^{o}C. The XRD patterns of the samples obtained at 600-900 ^{o}C for 1h are shown in Fig. 2. It is found that the peak intensity of the obtained sample tends to increase with the increase of reaction temperature. The increase in the intensity of diffraction peaks is attributed to the increase in the crystallinity of the obtained powder.

The SEM micrographs of $W_{0.97}Mo_{0.03}Se_2$ powder prepared at different reaction temperature are presented in Fig. 3. When the reaction temperature is 600 ^{o}C, a large number of regular conelike microrods are observed and the microrods are composed of many nonosheets (Fig. 3a). With increase the reaction temperature to 700-800 ^{o}C, the shape of the microrod became irregular. In addition, some small particles are also observed (Fig. 3b and 3c). When the reaction temperature is up to 900 ^{o}C, the microrods gradually disappeared and transformed into hexagonal microplates (Fig. 3d).

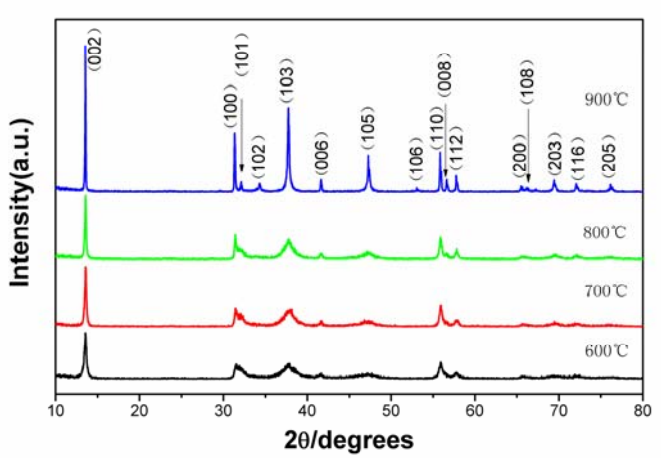

Fig. 2. XRD pattern of the products obtained at different temperature for 1 h.

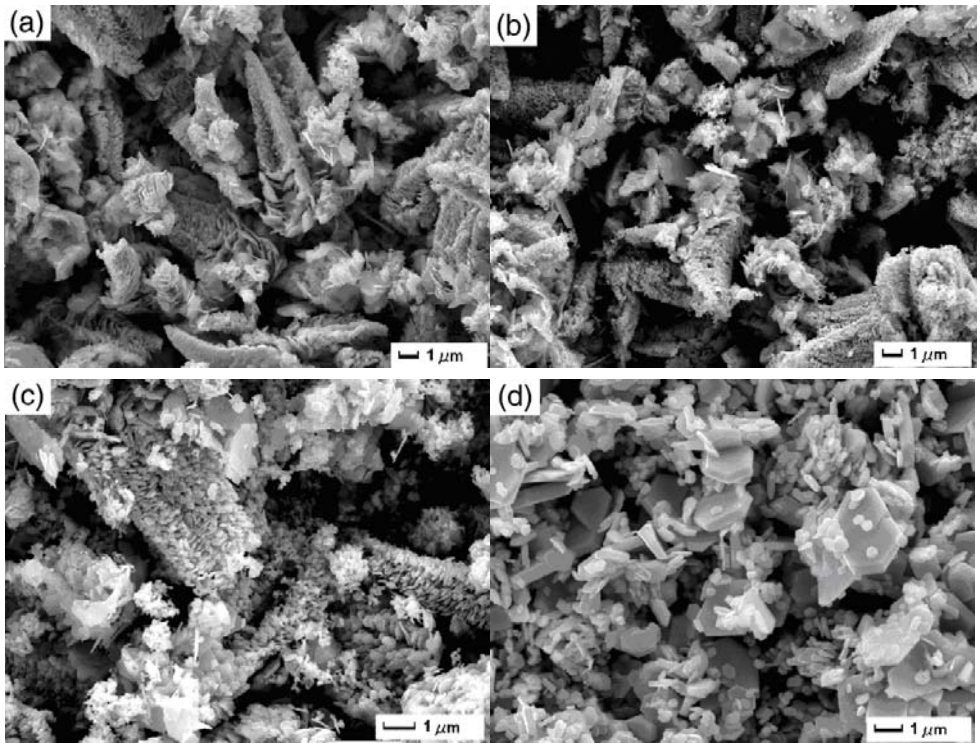

Fig.3. SEM of the products obtained at (a) 600 ^{o}C, *(b) 700* ^{o}C, *(c) 800* ^{o}C, *and (d) 900* ^{o}C *for 1 h.*

To investigate the influence of reaction time on the morphology of the final products, the samples obtained at different reaction time were analysed. The XRD patterns of the samples prepared at 750 ^{o}C for 30 min-12 h are shown in Fig. 4. After of 30 min reaction, part of unreacted tungsten powder were remained in the sample. With increasing the reaction time, all the tungsten powder transformed into $W_{0.97}Mo_{0.03}Se_2$ and the XRD peaks of the resultant products became stronger and sharper, suggesting the increase of their crystal sizes.

The morphology of the $W_{0.97}Mo_{0.03}Se_2$ samples obtained with different reaction time are presented in Fig. 5. It is observed that the size of $W_{0.97}Mo_{0.03}Se_2$ nanosheet increases with increasing the reaction time. As shown in Fig. 5a, the as-preapred $W_{0.97}Mo_{0.03}Se_2$ products with reaction time of 30 min were mainly composed of a large amount of aggregated nanosheets. With increasing the reaction time to 2 h, some hexagonal nanoplates and nanorods began to emerge (Fig. 5b). Upon increasing the reaction time to 4 h, more hexagonal nanoplates with larger size were formed and the number of aggregated nanoplates continued to decrease (Fig. 5c). When the reaction time was increased to 12 h, some irregular particles were formed and the original aggregated nanoplates disappeared.

From the observation made above, it is clear that the morphology of the obtained samples were affected by the reaction temperature and time greatly. The aggregated nanoplates with smaller size were obtained at lower temperature or shorter reaction time. The reason may be that the growth rate of the nucleus at this condition is very slowly. The increase in particle size is probably ascribed to the enhancing the reaction temperature and prolonging the reaction time. High temperature promotes the formation of nuclei and the longer reaction time promotes the growth of the nuclei.

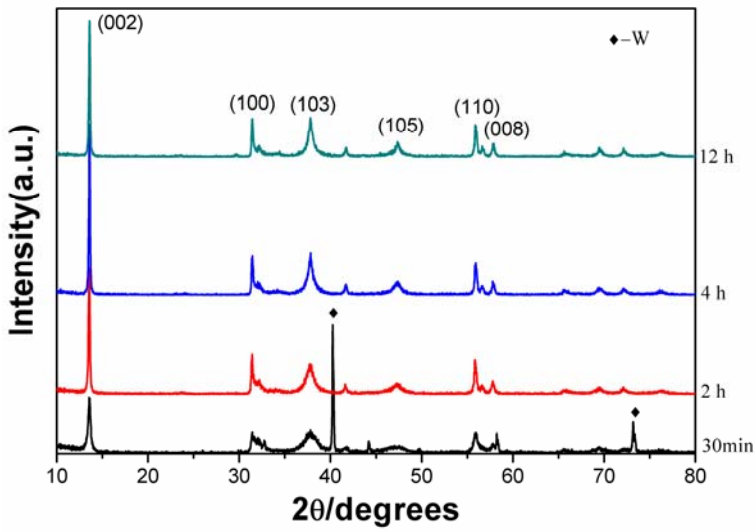

Fig. 4. XRD pattern of the products obtained at 750 °C for 30 min -12 h.

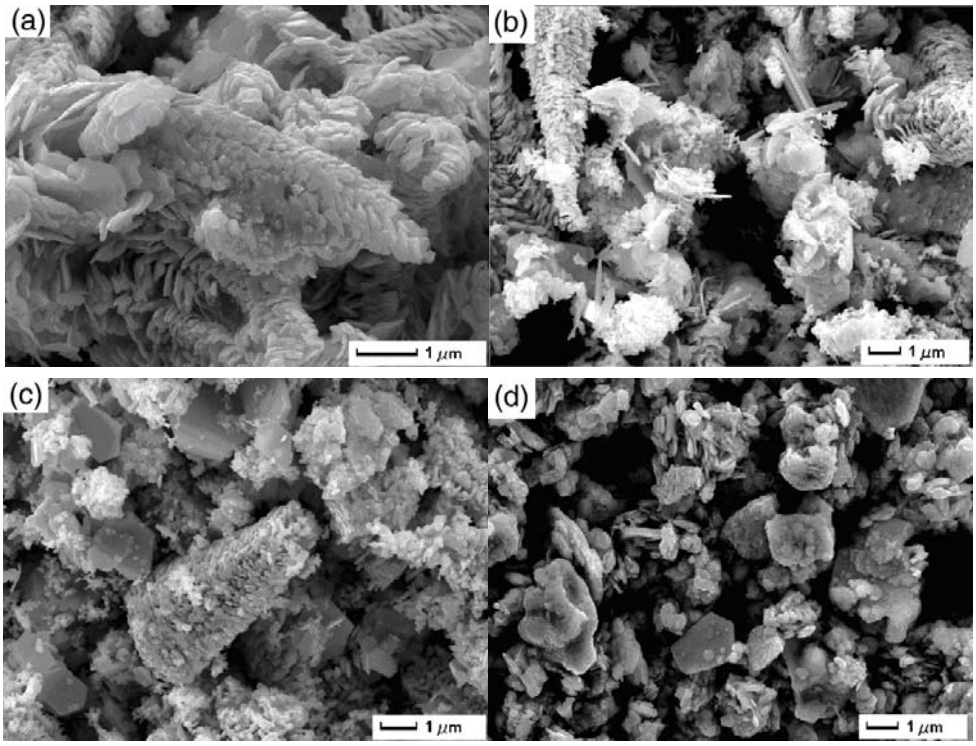

Fig. 5. SEM of the products obtained at 750 °C for (a) 30 min, (b) 2 h, (c) 4 h, and (d) 12 h.

3.3 Tribological properties analysis

Fig. 6a shows variations of friction coefficient of lubricant with different cotent of $W_{0.97}Mo_{0.03}Se_2$ with 40 N load and 400 rpm rotating speed. It could easily be found from Fig. 6a that friction coefficient is decreasing with the addition of $W_{0.97}Mo_{0.03}Se_2$ nanosheets. The friction coefficient of the base oil with 5 wt.% $W_{0.97}Mo_{0.03}Se_2$ nanoplates was stable and lower than that of the base oil with other content. The average friction coefficient of base oil with 5 wt.%

$W_{0.97}Mo_{0.03}Se_2$ nanosheets was close to 0.06, whereas it was 0.9 for the HVI500 base oil. That meant the addition of 5 wt.% $W_{0.97}Mo_{0.03}Se_2$ nanosheets to the base oil resulted in nearly 33.3% reduction for the friction coefficient of the base oil. Figure 6b shows the impact of load for the base oil containing 5 wt.% $W_{0.97}Mo_{0.03}Se_2$ nanosheets with 400 rpm rotating speed. Obviously, the friction coefficient at low load was lower than that at high load.

From the above results, $W_{0.97}Mo_{0.03}Se_2$ nanosheets as lubrication additive could improve tribological properties of the base oil. The lubrication mechanism of layered $W_{0.97}Mo_{0.03}Se_2$ nanosheet is associated with the shearing of the weak van der Waals bonds between the molecular layers. When $W_{0.97}Mo_{0.03}Se_2$ was used as an additive in a base-oil, besides molecules of the base oil, $W_{0.97}Mo_{0.03}Se_2$ powder was also adsorbed on the surface of the steel friction pair. The adsorbed $W_{0.97}Mo_{0.03}Se_2$ was able to endure a high load and improve the tribological properties of the base oil. The layered $W_{0.97}Mo_{0.03}Se_2$ reduced the friction between the friction pair through its shearing of layers [10].

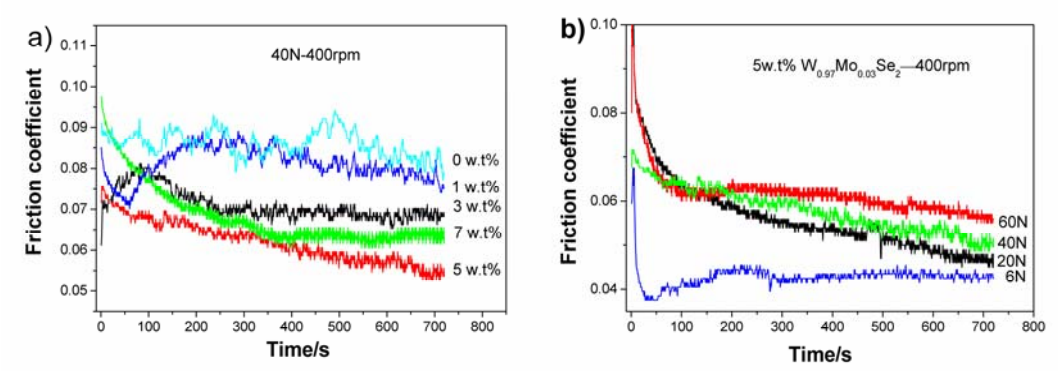

Fig. 6. Variation of friction coefficient for (a) the HVI500 base oil and the HVI500 base oil containing 1,3, 5, 7 wt.% $W_{0.97}Mo_{0.03}Se_2$ nanoplates at 40 N, (b) the HVI500 base oil containing 5 wt.% $W_{0.97}Mo_{0.03}Se_2$ nanoplates for 12 min.

4. Conclusion

In summary, the $W_{0.97}Mo_{0.03}Se_2$ nanosheets have been successfully prepared by solid state reaction. The results suggest that the morphologies of the as-prepared nanosheets affected by the reaction temperature and time. The introduction of $W_{0.97}Mo_{0.03}Se_2$ nanosheets as lubrication additives improves the tribological properties of the base oil. The friction coefficient of the base oil decreased with the mass percentage of the $W_{0.97}Mo_{0.03}Se_2$ additives increasing. The base oil with 5.0 wt.% $W_{0.97}Mo_{0.03}Se_2$ nanosheets presents better anti-wear capability than others.

Acknowledgements

This work was financially supported by National Natural Science Foundation of China (51275213, 51302112), the Jiangsu National Nature Science Foundation (BK2011534, BK2011480), the Jiangsu Industry-University-Research Joint innovation Foundation (BY213065-05, BY213065-06) and Scientific and Technological Innovation Plan of Jiangsu Province in China (Grant Nos. CXLX12_0636).

References

[1] F. Chinas-Castillo, H. A. Spikes. Trans. ASME. **125**, 522 (2003).

[2] J. Zhou, J. Yang, Z. Zhang, W. Liu, Q. Xue. Mater. Res. Bull. **34**, 1361 (1999).

[3] L. Rapoport, Y. Feldman, M. Homyonfer, H. Cohen, J. Sloan. Wear. **225**, 975 (1999).

[4] S. Chen, W. Liu, L. Yu. Wear. **218**, 153 (1998).

[5] B. Li, X. Wang, W. Liu, Q. Xue. Tribol. Lett. **22**, 79 (2006).

[6] L. Margulies, G. Salitra, R. Tenne, M. Talianker. Nature. **365**, 113 (1993).

[7] L. Rapoport, Y. Bilik, Y. Feldman, M. Homyonfer, S. R. Cohen, R. Tenne. Nature. **387**, 791 (1997).

[8] L. Rapoport, M. Lvovsky, I. Lapsker, V. Leshchinsky, Y. Feldman, R. Tenne. Wear. **249**, 149 (2001).

[9] K.H. Hu, M. Liu, Q.J. Wang, Y.F. Xu, S. Schraube, X.G. Hua. Tribol. Int. **42**, 33 (2009).

[10] J. H. Yang, H. X. Yao, Y. Q. Liu, Y. J. Zhang. Nanoscale Res. Lett. **3**, 481 (2008).

[11] K. Cao, C. S. Li, Y. H. Cheng, H. Tang, F. Y. Yan, H. J. Song. Tribol. T. **55**, 297(2012).

[12] C. S. Li, M. D. Hao, Y. Q. Liu, Y. Yu. presented at the 3rd IEEE International Conference on Nano/Miro Engineered and Molecular Systems, 2008, Sanya, China.

[13] H. Tang, C. S. Li, X. F. Yang, C. C. Mo, K. S. Cao, F. Y. Yan. Cryst. Res. Technol. **46**, 400 (2011).

[14] I. Efeoglu, O. Baran, F. Yetim, S. Altntas. Surf. Coat. Tech. **203**, 766 (2008).

[15] W. J. Li, L. F. Hu, M. Z. Wang, H. Tang, C. S. Li, J. Q. Liang, Y. Jin. Cryst. Res. Technol. **47**, 878(2012).

[16] X. H. Zhang, H. Tang, C. S. Li, S. Chen. Chalcogenide Lett. **10**, 403(2013).